RESEARCH   **Open Access**

Optimal receiver antenna location in indoor environment using dynamic differential evolution and genetic algorithm

Shu-Han Liao[1], Chien-Hung Chen[2], Chien-Ching Chiu[1*], Min-Hui Ho[1], Tadeusz A Wysocki[3] and Beata J Wysocki[3]

Abstract

Using the impulse responses of these multipath channels, the bit error rate (BER) performance for binary pulse amplitude modulation impulse radio ultra-wideband communication system is calculated. The optimization location of receiving antenna is investigated by dynamic differential evolution (DDE) and genetic algorithm (GA) to minimize the outage probability. Numerical results show that the performance for reducing BER and outage probability by DDE algorithm is better than that by GA.

Keywords: BER; BPAM; UWB; DDE; GA

1 Introduction

Ultra-wideband (UWB) transmissions can legally operate in the range from 3.1 up to 10.6 GHz at a limited transmit power of −41 dBm/MHz [1]. All wireless systems must be able to deal with the challenges of operating over a multipath propagation channel, where the object in the environment can cause multiple reflections. Bit error rate (BER) degradation is caused by the inter-symbol interference due to a multipath propagation made up of radio wave reflections by walls, ceilings, floors, and office fixtures. In general, effective antenna selection and deployment strategies are important for reducing BER in indoor wireless systems [2,3]. To the best of our knowledge, there is still no investigation using the dynamic differential evolution (DDE) and genetic algorithm (GA) to optimize the location of receiving antennas for minimizing the BER in indoor wireless communication channel.

Based on the BER formula, the outage probability is chosen as the cost function in our optimization procedure. Thus, the optimization of location of receiving antenna in this paper is using DDE and GA to overcome the above situation and to minimize the outage probability.

The remainder of this paper is organized as follows: In Section 2, channel modeling, system description, dynamic differential evolution, and genetic algorithm procedure are presented. The numerical results are then presented in Section 3, and conclusion is made in Section 4.

2 Channel modeling and system description

2.1 Channel modeling

The following two steps are used to calculate the multipath radio channel:

1. *Frequency responses for sinusoidal waves by shooting and bouncing ray (SBR)/image* [4-23] *techniques.* The SBR/image method can deal with high-frequency radio wave propagations in the complex indoor environments [24,25].

2. *Inverse fast Fourier transform (IFFT) and Hermitian processing.* The frequency responses are transformed to the time domain using the inverse Fourier transform with the Hermitian signal processing [26]. Using the Hermitian processing, the pass-band signal is obtained with zero padding from the lowest frequency down to direct current (DC), taking the conjugate of the signal and reflecting it to the negative frequencies. The result is then transformed to the time domain using IFFT [27]. Since the signal spectrum is symmetric around DC. The resulting doubled-side spectrum corresponds to a real signal in the time domain.

* Correspondence: chiu@ee.tku.edu.tw
[1]Department of Electrical Engineering, Tamkang University, Tamsui District, New Taipei City 251, Taiwan
Full list of author information is available at the end of the article

The equation for modeling the multipath radio channel is a linear filter with an impulse response given by

$$h(t) = \sum_{n=1}^{N} \alpha_n \delta(t-\tau_n), \tag{1}$$

where N is the number of paths observed at time, $\delta(\cdot)$ is the Dirac delta function, and a_n and τ_n are the channel gain and time delay for the n-th path, respectively.

2.2 System block diagram

The block diagram of the simulated communication system is shown in Figure 1. The received signal $r(t)$ can be expressed as follows:

$$r(t) = [x(t) \otimes h(t)] + n(t), \tag{2}$$

where $x(t)$ is the transmitted signal, $h(t)$ is the impulse response of the equivalent baseband, and $n(t)$ is the white Gaussian noise with zero mean and variance $N_0/2$.

The transmitted UWB pulse stream can be expressed as follows [28]:

$$x(t) = \sum_{n=1}^{\infty} p[t-(n-1)T_d]d_n, \tag{3}$$

where $p(t)$ is the transmitted waveform. $d_n \in \{\pm1\}$ is a binary pulse amplitude modulation (B-PAM) symbol and is assumed to be independent and identically distributed. T_d is the duration of the transmitting signal. The transmitted waveform $p(t)$ is the Gaussian waveform with ultra-short duration T_p at the nanosecond scale. Note that T_d is the duration of the transmitting signal, and T_p is the pulse duration. The value of T_d is usually much larger than that of T_p. The Gaussian waveform $p(t)$ can be described by the following expression:

$$p(t) = \frac{1}{\sqrt{2\pi}\sigma} e^{\frac{-t^2}{2\sigma^2}}, \tag{4}$$

where t and σ are time and standard deviation of the Gaussian wave, respectively. The average transmit energy symbol E_t can be expressed as

$$E_t = \int_0^{T_d} p^2(t)dt, \tag{5}$$

where E_t is the average transmitted energy.

The correlation receiver samples the received signal at the symbol rate and correlates them with suitably delayed references given by

$$q(t) = p[t-\tau_1-(n-1)T_d], \tag{6}$$

where τ_1 is the delay time of the first wave. The output of the correlator at $t = nT_d$ is [29,30]:

$$Z(n) = \int_{(n-1)T_d}^{nT_d} \left\{ \left[\sum_{n=1}^{\infty} p[t-(n-1)T_d]d_n \right] \otimes h(t) \right\}$$
$$\cdot q(t)dt + \int_{(n-1)T_d}^{nT_d} n(t)q(t)dt$$
$$= V(n) + \eta(n). \tag{7}$$

It can be shown that the noise components $\eta(n)$ of Equation 7 are uncorrelated Gaussian random variables with zero mean. The variance of the output noise η is

$$\sigma^2 = \frac{N_0}{2} E_t. \tag{8}$$

The conditional error probability of the n-th bit is thus expressed by

$$P_e\left[Z(n) \middle| \vec{d} \right] = \frac{1}{2} \text{erfc}\left[\frac{V(n)}{\sqrt{2}\sigma} \cdot (d_n) \right], \tag{9}$$

where $\text{erfc}(x) = \frac{2}{\sqrt{\pi}} \int_x^{\infty} e^{-y^2} dy$ is complementary error function and $\left\{ \vec{d} \right\} = \{d_0, d_1, ..., d_n\}$ is the binary sequence. Note that the average BER for B-PAM impulse radio UWB system can be expressed as [10]

$$\text{BER} = \sum_{i=1}^{2^n} P\left(\vec{d} \right) \cdot \frac{1}{2} \text{erfc}\left[\frac{V(i)}{\sqrt{2}\sigma} \cdot (d_n) \right], \tag{10}$$

where $P\left(\vec{d} \right)$ is the occurring probability of the binary sequence $\vec{d}$.

2.3 Dynamic differential evolution

In dynamic differential evolution (DDE), after generating the initial population, the candidate solutions are refined by applying mutation, crossover, and selection, iteratively. The flowchart of the DDE algorithm is shown in Figure 2. In this strategy, a mutant vector for each target vector V_j^{k+1} at the $k + 1$ generation is computed by

$$\left(V_j^{k+1} \right)i = \left(X_j^k \right)i + \zeta \cdot \left[(X_{\text{best}}^k)i - \left(X_j^k \right)i \right] + \chi \cdot \left[(X_m^k)i - (X_n^k)i \right],$$
$$j, m, n \in [0, N_p-1], \quad m \neq n, \tag{11}$$

where $i = 1 \sim D$ and χ and ζ are the scaling factors associated with the vector differences $\left(X_{\text{best}}^k - X_j^k \right)$ and $\left(X_m^k - X_n^k \right)$, respectively. The disturbance vector V due to the mutation mechanism consists of parameter vector X_j^k, the best particle X_{best}^k, and two randomly selected vectors. As comparison, the mutant vector V_j^{k+1} is generated according to Equation 12 for typical DE [31]:
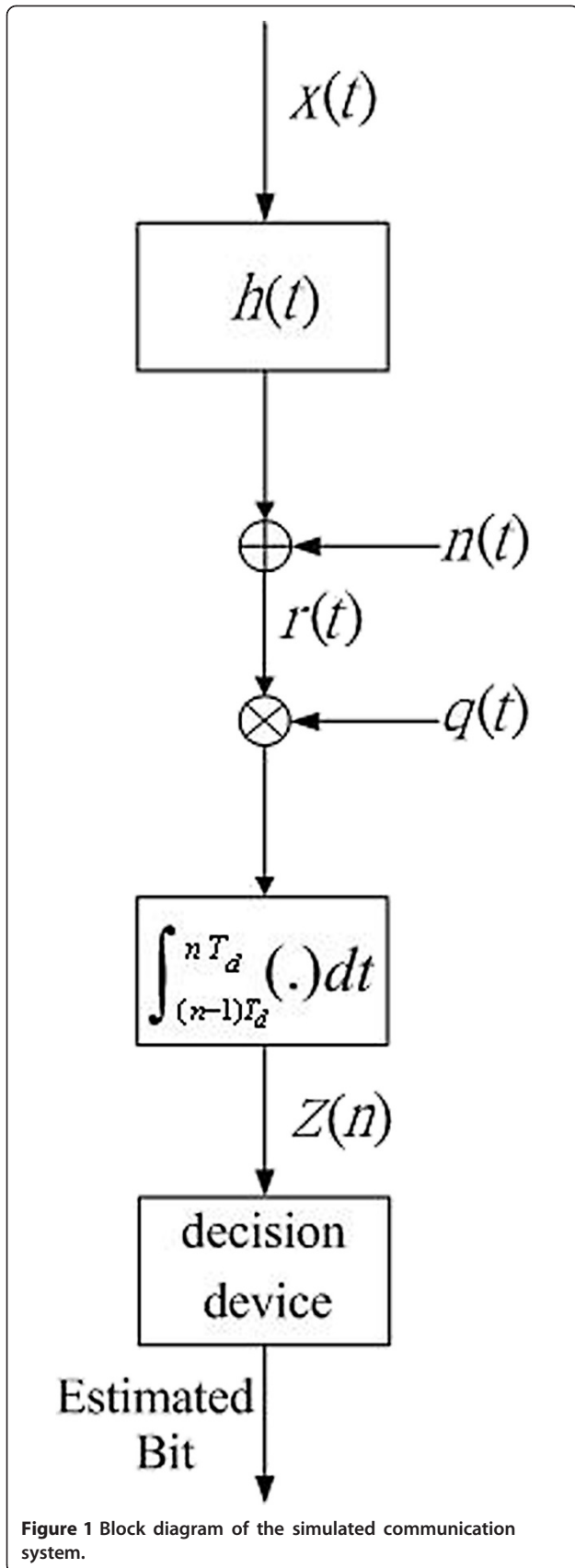
Figure 1 Block diagram of the simulated communication system.

$$\left(V_j^{k+1}\right)i = \left(X_j^k\right)i + \chi \cdot \left[\left(X_m^k\right)i - \left(X_n^k\right)i\right],$$
$$j, m, n \in [0, N_p - 1], \quad m \neq n, \tag{12}$$

where $i = 1 \sim D$ and χ is the scaling factor associated with the vector difference $\left(X_m^k - X_n^k\right)$. Note that ζ is set to 0 for DE; therefore, the main differences between DDE and DE is that DDE includes the idea of approaching the 'best' during the course of optimization procedure.

After mutation, the crossover operator is applied to generate another kind of new vector u_j. The crossover operation in DDE delivers the crossover vector u_j^{k+1} by mixing the components of the current vector X_i and the above mutant vector V_i. It can be expressed as

$$u_j^{k+1} = \begin{cases} \left(V_j^{k+1}\right)_i, & Q_k < \mathrm{CR} \\ \left(X_j^k\right)_i, & Q_k \geq \mathrm{CR}, \end{cases} \tag{13}$$

where $i = 1 \sim D$ and Q_k is a random number uniformly distributed within [0,1]. $\mathrm{CR} \in (0, 1)$ is a predefined crossover rate. DDE uses a greedy selection operator that is defined by

$$X_j^{k+1} = \begin{cases} u_j^{k+1}, & \text{if } \mathrm{CF}\left(u_j^k\right) < \mathrm{CF}\left(X_j^k\right) \\ X_j^k, & \text{otherwise.} \end{cases} \tag{14}$$

Selection operation is conducted by comparing the parent vector X_j^{k+1} with the crossover vector u_j^{k+1}. The vector with smaller cost function (CF) value is selected as a member for the next generation.

In the synthesis procedure, the DDE is used to minimize the following CF:

$$\mathrm{CF} = \text{outage probability}, \tag{15}$$

where cost function is the outage probability for UWB system. The outage probabilities for 100-Mbps B-PAM and for a BER $< 10^{-3}$ versus SNR are calculated. DDE is used to search the receiver antenna location to minimize the outage probability of the communication system. This SBR/image method technique is used to calculate the UWB channel impulse response for each location of the receiver. Based on the channel impulse response, the number of multipath components, the root mean square (RMS) delay spread τ_{RMS}, and the mean excess delay τ_{MED} are computed. The DDE algorithm iteratively generates a new population that springs from the previous population through the application of the reproduction by mutation and replacement operators. In our simulation, when the cost function is bigger than the threshold
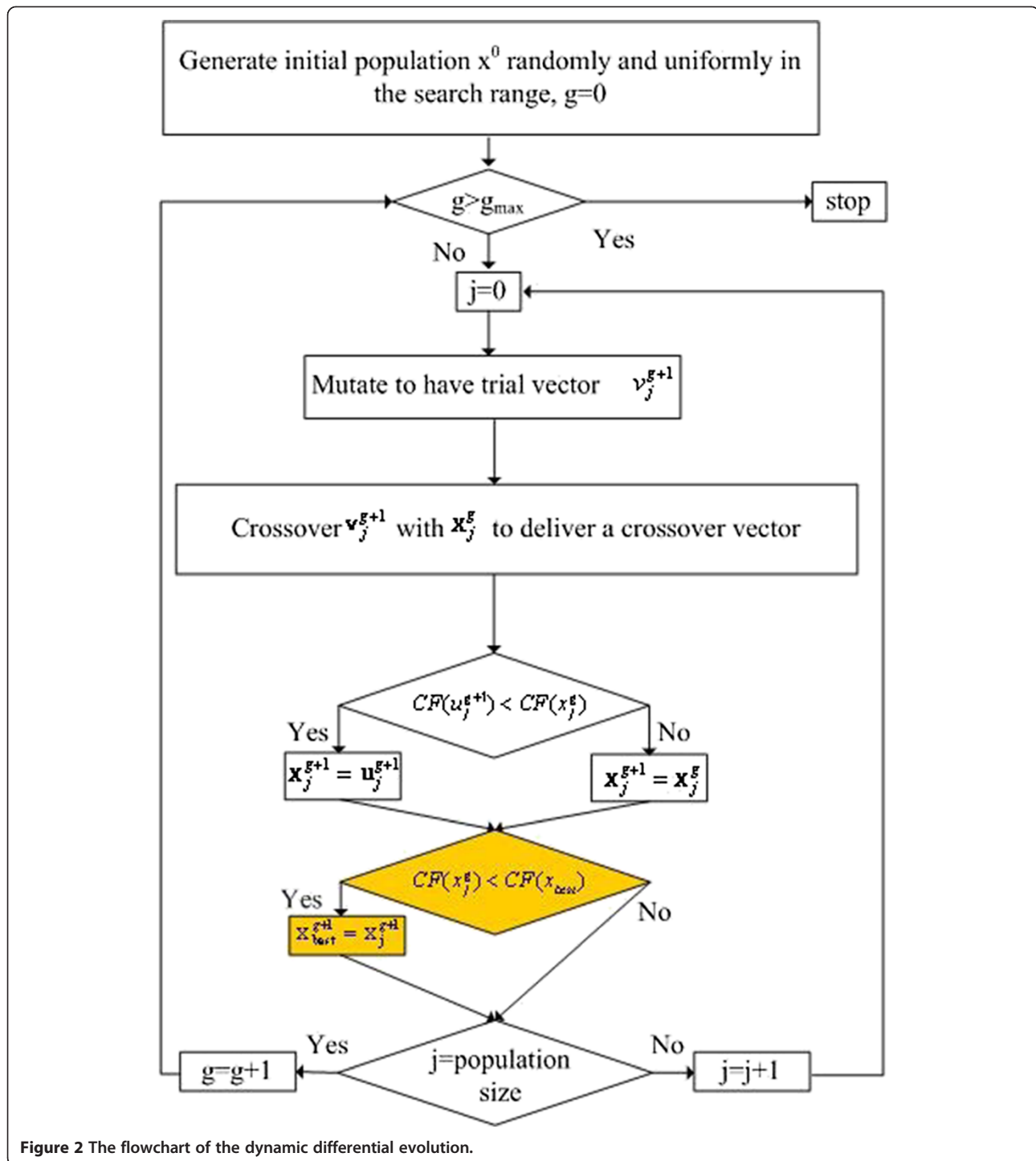
Figure 2 The flowchart of the dynamic differential evolution.

value or DDE does not find a better individual within 300 successive generations, the DDE will be terminated, and a solution is then obtained.

2.4 Genetic algorithm

Genetic algorithm (GA) is the global numerical optimization methods based on genetic recombination and evaluation in nature [32,33]. They use the iterative optimization procedures, which start with a randomly selected population of potential solutions and then gradually evolve toward a better solution through the application of the genetic operators. GA typically operates on a discretized and coded representation of the parameters rather than on the parameters themselves. These representations are often considered to be

'chromosomes', while the individual element, which constitutes chromosomes, is the 'gene'. Simple but often very effective chromosome representations for optimization problem involving several continuous parameters can be obtained through the juxtaposition of discretized binary representations of the individual parameter.
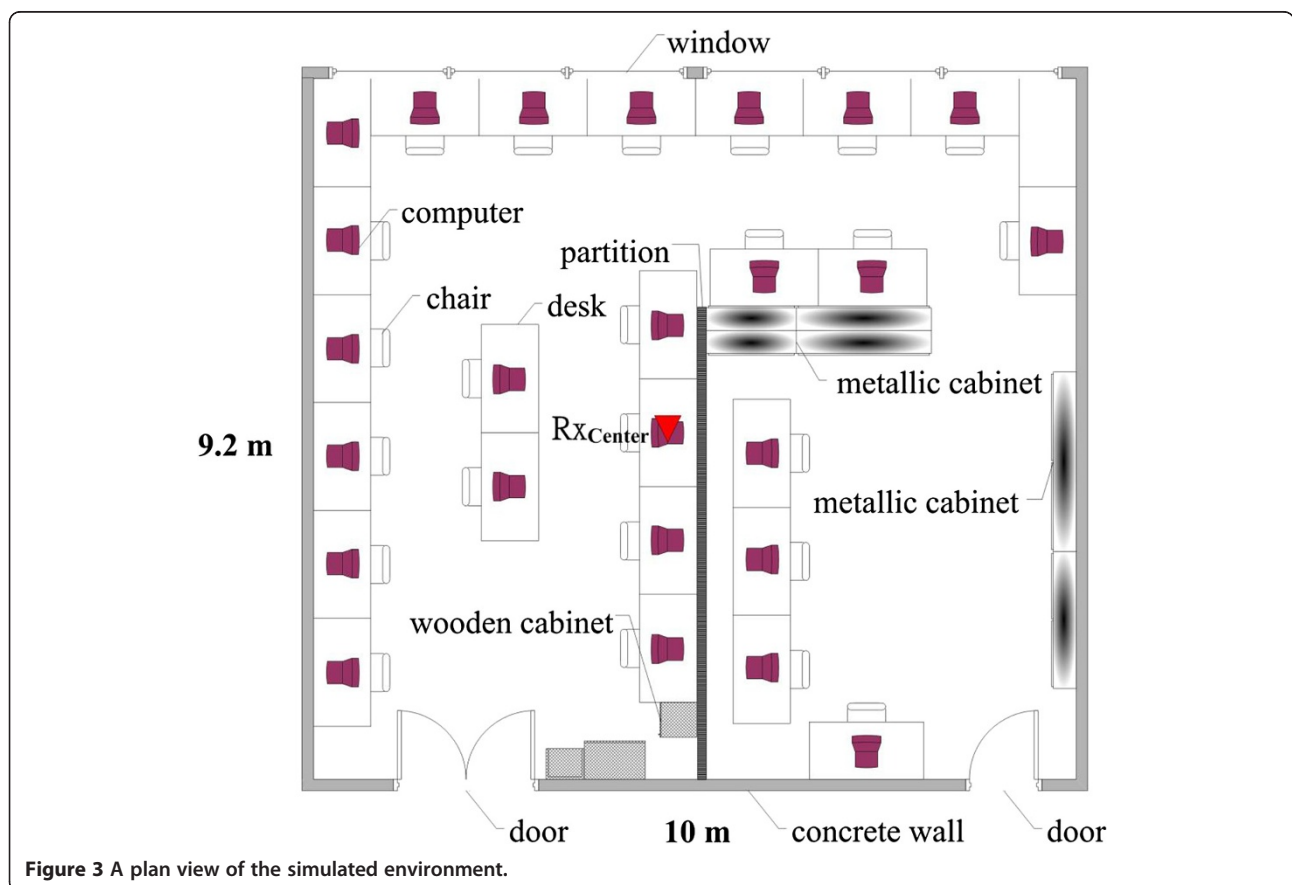
We regulate the receiver antenna location of the indoor environment to minimize the outage probability. The GA starts with a population containing a total of G_P candidates (i.e., G_P is the population size). Each candidate is described by a chromosome. Then, the initial population can simply be created by taking G_P random chromosomes. GA iteratively generates a new population, which is derived from the previous population through the application of the reproduction, crossover, and mutation operators.
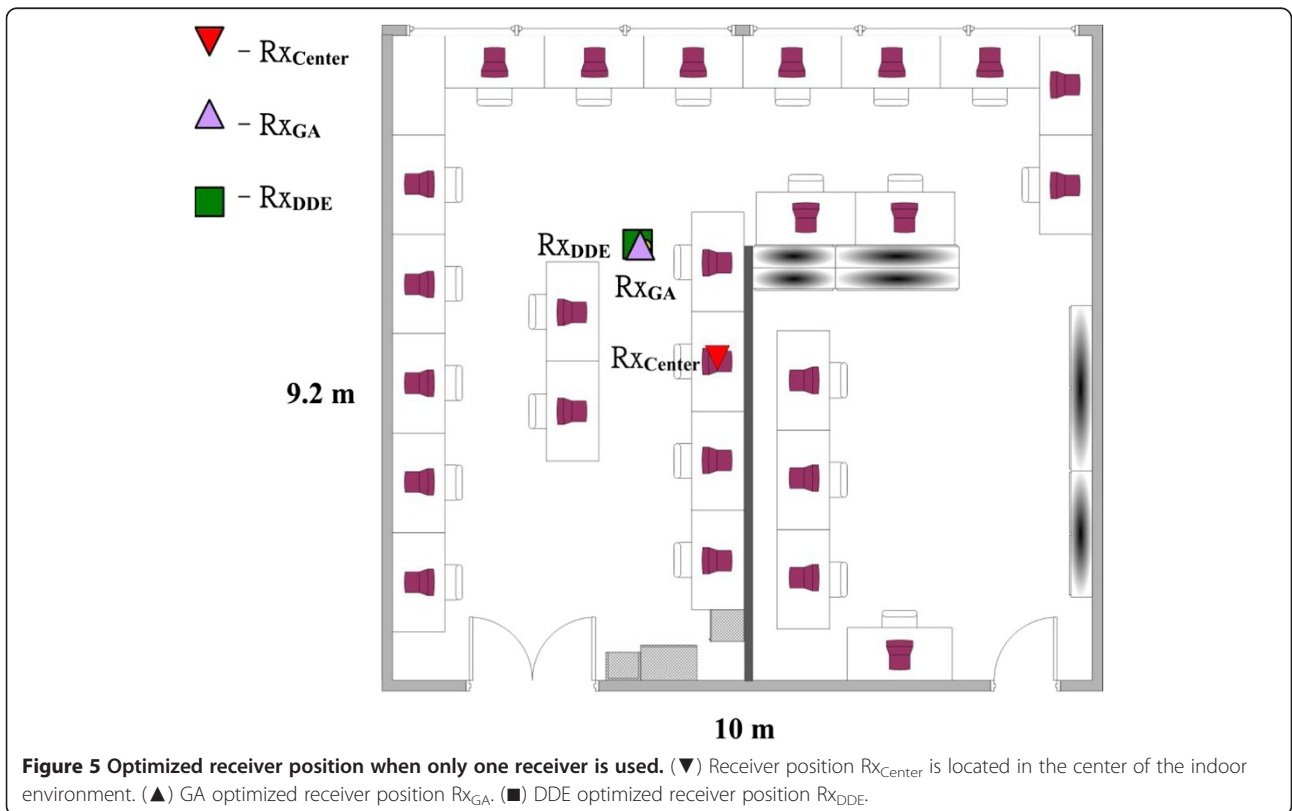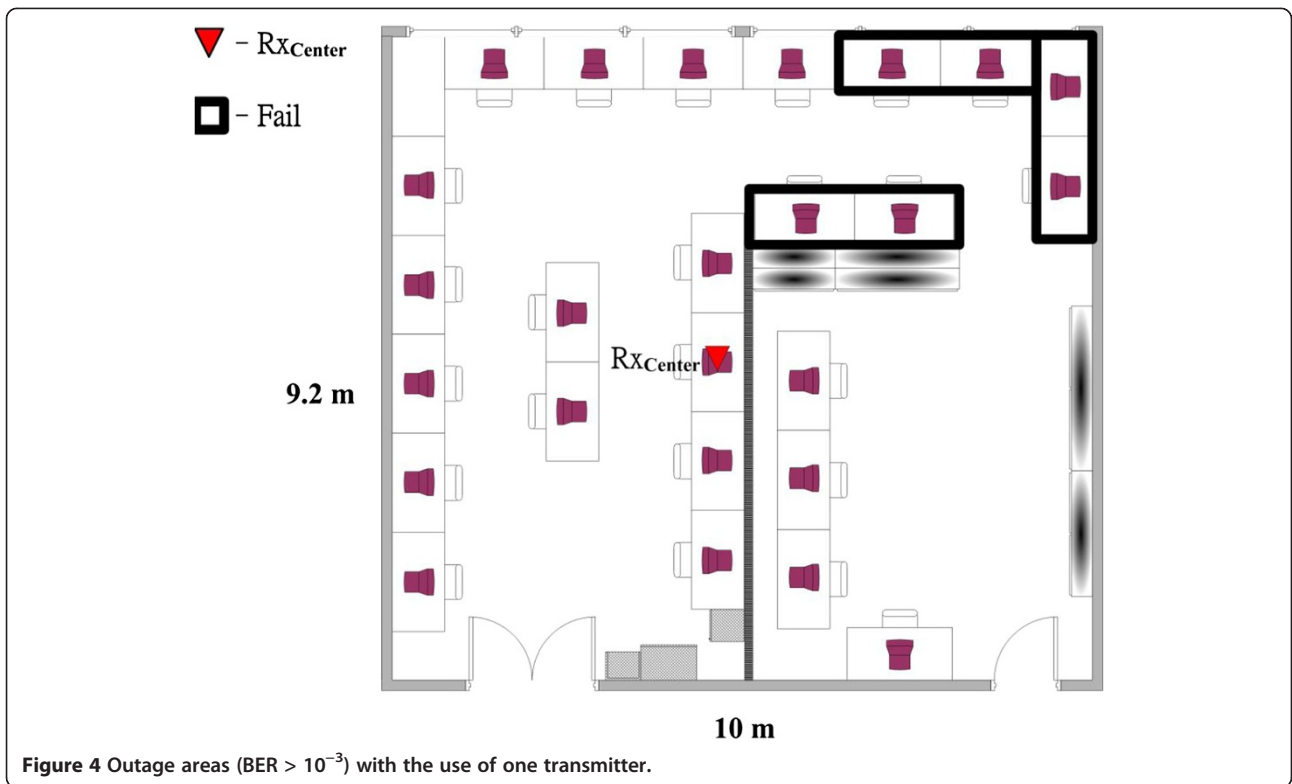
The GA is used to minimize the cost function in Equation 15, where cost function is the outage probability for UWB system. Through repeated applications of reproduction, crossover, and mutation operators, the initial population is transformed into a new population in an iterative manner. New populations will contain increasingly better chromosomes and will eventually converge to an optimal population that consists of the optimal chromosomes.

As for the GA calculations, each chromosome is assigned information of the position of transmitter as the optimization variables. For each generated chromosome, the GA reruns the ray tracing program to calculate the BER for each receiver from the given location of transmitter provided by the chromosome. In our simulation, when the BER is lower than the threshold value or GA does not find a better individual within 300 successive generations, the GA will be terminated and a solution is then obtained.

3 Numerical results

A ray tracing technique is developed to calculate the channel impulse response from 3.1 to 10.6 GHz with frequency interval of 5 MHz, i.e., 1,501 frequency components are used. Since the dielectric constant and conductivity of the materials change with frequency, the different values of dielectric constant and conductivity of materials for different frequencies are carefully considered in channel calculation [34-37]. The BER for different receiver positions in the indoor environments are investigated. Figure 3 is the top view of the indoor environment with dimensions of 10 m (length) × 9.2 m (width) × 3 m (height). The transmitting and receiving antennas are with simple omnidirectional radiation pattern and vertically

Figure 3 A plan view of the simulated environment.

Figure 4 Outage areas (BER > 10^{-3}) with the use of one transmitter.

Figure 5 Optimized receiver position when only one receiver is used. (▼) Receiver position Rx_{Center} is located in the center of the indoor environment. (▲) GA optimized receiver position Rx_{GA}. (■) DDE optimized receiver position Rx_{DDE}.

polarized. Each antenna is with a fixed height of 1 m. The optimal antenna location for minimizing the outage probability is searched by DDE and GA. The relative coefficients of the DDE are set as follows: The scaling factors of F and λ are both 0.8, and the crossover rate CR = 0.6. The population size N_p = 30. The relative coefficients of the GA are set as follows: The crossover rate G_r = 0.6. The mutation probability G_M = 0.025, and the population size G_P = 30. The cases with different transceiver positions are considered in our simulation. The receiving antenna Rx_{Center} (5 m × 4.6 m × 0.73 m) located in the center of the indoor environment with a fixed height of 1 m is used for our reference, as shown in Figure 3.

Based on the channel impulse response, the number of multipath components, the RMS delay spread τ_{RMS}, and the mean excess delay τ_{MED} are computed. The cumulative distributions of the RMS delay spread τ_{RMS} is defined as [38]

$$\tau_{RMS} = \sqrt{\frac{\sum_{n=1}^{N} \tau_n^2 |a_n|^2}{G} - \left(\frac{\sum_{n=1}^{N} \tau_n |a_n|^2}{G}\right)^2}, \quad (16)$$

where $G = \sum_{n=1}^{N} |a_n|^2$ is the total multipath gain.

The mean excess delay, τ_{MED}, is defined as [39]

$$\tau_{MED} = \frac{\sum_{n=1}^{N} \tau_n |a_n|^2}{G} \quad . \quad (17)$$

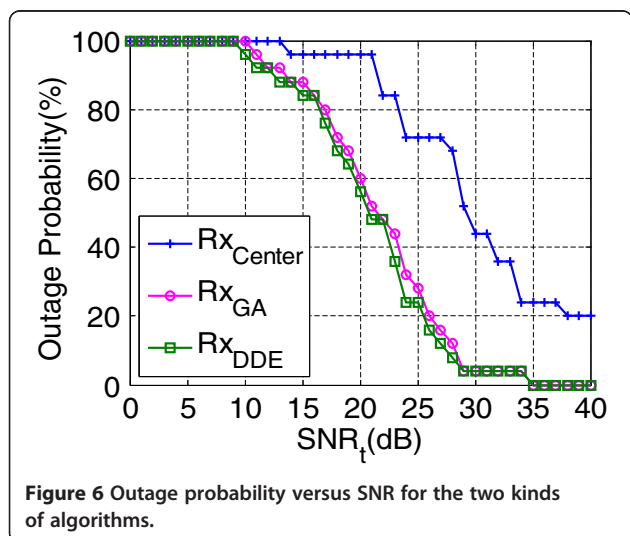By Equations 16 and 17, we can obtain the RMS delay spreads and mean excess delay.

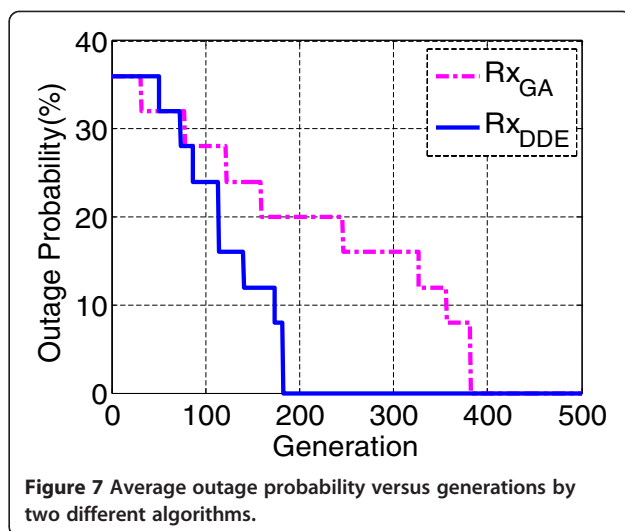**Figure 6 Outage probability versus SNR for the two kinds of algorithms.**

Figure 7 Average outage probability versus generations by two different algorithms.

We compare the effects of Rx_{Center}, Rx_{DDE}, and Rx_{GA} on UWB transmission. For the case, the receiver is mobile in the whole indoor environment and the transceivers are located on the desk, in which 25 measurements are carried out (e.g., transmission from a computer 'Tx' to a printer 'Rx'). Figure 4 shows that the transmitting antenna Rx_{Center} (5 m × 4.6 m × 0.73 m) is located in the center of the indoor environment. In this case, six bad receiving signal points (BER > 10^{-3}) occurred including (not highlighted in the figure) the transmitter points. The DDE and GA optimization position of the receiver is shown in Figure 5. The optimal locations of the receiving antennas are at Rx_{DDE} (3.52 m × 6.25 m × 0.73 m) and Rx_{GA} (3.56 m × 6.24 m × 0.73 m) using the DDE and GA, respectively. The optimization receiver points Rx_{DDE} and Rx_{GA} are chosen as the receiver locations as squares/triangle, and no bad transmitting signal point exists. The outage probability versus SNR is calculated, as shown in Figure 6. Here, SNR is defined as the ratio of the average transmitted power to the noise power at the front end of the receiver. It is seen that the outage probability at SNR = 28 dB are about 68%, 8%, and 12% for Rx_{Center}, Rx_{DDE}, and Rx_{GA}, respectively. It is clear that the outage probability decreased by DDE is better than those by GA about 50%. The performance for the antenna location by DDE is better than that by GA.

Table 1 The channel parameters (τ_{MED} and τ_{RMS}) for the two kinds of algorithms

	Transmitter channel parameters	
	τ_{MED} (ns)	τ_{RMS} (ns)
Rx_{Center}	7.64	12.50
Rx_{GA}	2.86	7.12
Rx_{DDE}	2.80	6.69

The outage probability versus generation DDE and GA are calculated, as shown in Figure 7. It is found that the outage probability decreases quickly by the DDE, and good convergences are achieved within 182 generations. It also shows that the convergent speed for the DDE is faster than that for GA.

In order to determine the multipath effect, the τ_{RMS} and τ_{MED} were calculated. A summary of these values are given in Table 1 for scenarios. For the transceivers located on the table's case scenario, the τ_{RMS} for Rx_{Center}, Rx_{DDE}, and Rx_{GA} are 12.5, 2.80, and 2.86 ns, respectively. It is clear that the τ_{RMS} for the Rx_{Center} case is the biggest.

4 Conclusions

Using the impulse responses of these multipath channels, the BER performance for UWB communication system is calculated. The DDE and GA are used to minimize the BER. Numerical results show that BER in the cases can be decreased. It is also found that the BER decreased by DDE is better than that by GA. Numerical results also show that the DDE outperforms the GA in convergence speed.

Author details
[1]Department of Electrical Engineering, Tamkang University, Tamsui District, New Taipei City 251, Taiwan. [2]Department of Computer and Communication Engineering, Taipei College of Maritime Technology, Danshui Town, New Taipei City 251, Taiwan. [3]Peter Kiewit Institute, University of Nebraska-Lincoln, Lincoln, NE 68588, USA.

References
1. Federal Communications Commission, *Revision of part 15 of the commission's rules regarding ultra-wideband transmission systems*. First report and order (FCC, Washington, DC, 2002)
2. AH Wong, MJ Neve, KW Sowerby, Antenna selection and deployment strategies for indoor wireless communication systems. IET Commun. **1**(4), 732–738 (2007)
3. DCK Lee, MJ Neve, KW Sowerby, The impact of structural shielding on the performance of wireless systems in a single-floor office building. IEEE Trans. on Wireless Comm. **6**(5), 1787–1795 (2007)
4. CC Chiu, CL Liu, SH Liao, Channel characteristics of ultra-wideband systems with single co-channel interference. Wirel. Commun. Mob. Comput. **13**(9), 864–873 (2013)
5. CC Chiu, CY Yu, SH Liao, MK Wu, Channel capacity of multiple-input multiple-output systems for optimal antenna spacing by particle swarm optimizer. Wirel. Pers. Commun. **69**(4), 1865–1876 (2013)
6. CC Chiu, CH Chen, SH Liao, KC Chen, Bit error rate reduction by smart UWB antenna array in indoor wireless communication. J. Appl. Sci. Eng. **15**(2), 139–148 (2012)
7. CC Chiu, CH Chen, SH Liao, TC Tu, Ultra-wideband outdoor communication characteristics with and without traffic. EURASIP J. Wirel. Commun. Netw. **2012**, 92 (2012)
8. CC Chiu, YT Kao, SH Liao, YF Huang, UWB communication characteristics for different materials and shapes of the stairs. J. Commun. **6**(8), 628–632 (2011)
9. SH Liao, HP Chen, CC Chiu, CL Liu, Channel capacities of indoor MIMO-UWB transmission for different material partitions. Tamkang J. Sci. Eng. **14**(1), 49–63 (2011)
10. CL Liu, CC Chiu, SH Liao, YS Chen, Impact of metallic furniture on UWB channel statistical characteristics. Tamkang J. Sci. Eng. **12**(3), 271–278 (2009)
11. SH Liao, CC Chiu, MH Ho, Comparison of dynamic differential evolution and genetic algorithm for MIMO-WLAN transmitter antenna location in indoor environment. Wirel. Pers. Commun. **71**(4), 2677–2691 (2013)
12. CC Chiu, MH Ho, SH Liao, MIMO-UWB smart antenna communication characteristics for different antenna arrays of transmitters. Int. J. RF and Microwave Computer-Aided Eng. **23**(3), 378–392 (2013)
13. CC Chiu, MH Ho, SH Liao, PSO and APSO for optimizing coverage in indoor UWB communication system. Int. J. RF and Microwave Computer-Aided Eng. **23**(3), 300–308 (2013)
14. SH Liao, CC Chiu, CH Chen, MH Ho, Channel characteristics of MIMO-WLAN communications at 60 GHz for various corridors. EURASIP J. Wirel. Commun. Netw. **2013**, 96 (2013)
15. MH Ho, CC Chiu, SH Liao, Comparison of different antenna arrays for the BER reduction in indoor wireless communication. Int. J. Commun. Syst. **26**(2), 161–176 (2013)
16. CH Sun, CC Chiu, MH Ho, CL Li, Comparison of dynamic differential evolution and self-adaptive dynamic differential evolution for buried metallic cylinder. Res. Nondestruct. Eval. **24**, 35–50 (2013)
17. MH Ho, CC Chiu, SH Liao, Optimization of channel capacity for MIMO smart antenna using particle swarm optimizer. IET Commun. **6**(16), 2645–2653 (2012)
18. MH Ho, CC Chiu, SH Liao, Bit error rate reduction for circular ultrawideband antenna by dynamic differential evolution. Int. J. RF and Microwave Computer-Aided Eng. **22**(2), 260–271 (2012)
19. SH Liao, MH Ho, CC Chiu, CH Lin, Optimal relay antenna location in indoor environment using particle swarm optimizer and genetic algorithm. Wirel. Pers. Commun. **62**(3), 599–615 (2012)
20. SH Liao, CC Chiu, MH Ho, CL Liu, Channel capacity of multiple-input multiple-output ultra wide band systems with single co-channel interference. Int. J. Commun. Syst. **23**(12), 1600–1612 (2010)
21. SH Liao, MH Ho, CC Chiu, Bit error rate reduction for multiusers by smart UWB antenna array. Prog. Electromagn. Res.C **16**, 85–98 (2010)
22. MH Ho, SH Liao, CC Chiu, UWB communication characteristics for different distribution of people and various materials of walls. Tamkang J. Sci. Eng. **13**(3), 315–326 (2010)
23. MH Ho, SH Liao, CC Chiu, A novel smart UWB antenna array design by PSO. Prog. Electromagn. Res.C **15**, 103–115 (2010)
24. SH Chen, SK Jeng, An SBR/image approach for indoor radio propagation in a corridor. IEICE Trans. Electron **E78-C**, 1058–1062 (1995)
25. SH Chen, SK Jeng, SBR/image approach for indoor radio propagation in tunnels with and without traffic. IEEE Trans. Veh. Technol. **45**, 570–578 (1996)
26. I Oppermann, M Hamalainen, J Iinatti, *UWB Theory and Applications* (Wiley, New York, 2004)
27. EW Kamen, BS Heck, *Fundamentals of Signals and Systems Using the Web and MATLAB* (Upper Saddle River, Prentice Hall, 2000)
28. T Zhi, GB Giannakis, BER sensitivity to mistiming in ultra-wideband impulse radios—part I: nonrandom channels. IEEE Trans. Signal Process. **53**, 1550–1560
29. EA Homier, RA Scholtz, *Rapid acquisition of ultra-wideband signals in the dense multipath channel*. IEEE Conference on Ultra Wideband System and Technologies, Baltimore, May 2002 (IEEE, Piscataway, 2002), pp. 105–109
30. DJ Gargin, *A fast and reliable acquisition scheme for detecting ultra wide-band impulse radio signals in the presence of multi-path and multiple access interference, International Workshop on Ultra Wideband System, May 2004* (Piscataway, IEEE, 2004). pp. 106–110
31. R Storn, K Price, *Differential evolution—a simple and efficient adaptive scheme for global optimization over continuous spaces, Technical report TR-95-012* (International Computer Science Institute, Berkeley, 1995)
32. DE Goldberg, *Genetic Algorithm in Search, Optimization and Machine Learning* (Addison-Wesley, Boston, 1989)
33. J Michael Johnson, Y Rahmat-Samii, Genetic algorithms in engineering electromagnetics. IEEE Antenn. Propag. Mag. **39**(4), 7–21 (1997)
34. Y Zhao, Y Hao, A Akram, P Clive, UWB on-body radio channel modeling using ray theory and subband FDTD method. IEEE Trans. Microw. Theor. Tech. **54**, 1827–1835 (2006)
35. RM Buehrer, A Safaai-Jazi, W Davis, D Sweeney, *Ultra-wideband propagation measurements and modeling*. Final report, DARPA NETEX Program Virginia Tech, 3rd edn., 2004, pp. 38–216
36. A Muqaibel, A Safaai-Jazi, A Bayram, AM Attiya, SM Riad, *Ultra-wideband through-the-wall propagation*. IEEE Proceedings Microwaves, Antennas and Propagation, December 2005 (IEEE, Piscataway, NJ, 2005), pp. 581–588

37. AS Jazi, SM Riad, A Muqaibel, A Bayram, Through-the-wall propagation and material characterization, DARPA NETEX Program Report, 2002
38. M Gabriella, D Benedetto, G Giancola, *Understanding Ultra Wide Band Radio Fundamentals* (Prentice Hall, Upper Saddle River, 2004)
39. TS Rappaport, *Wireless Communications: Principles and Practice*, 2nd edn. (Upper Saddle River, Prentice Hall, 2002)